A NOVEL RADIO-WAVE ALIGNMENT TECHNIQUE FOR MILLIMETER AND SUB-MILLIMETER RECEIVERS

C. -Y. E. Tong[1], M. T. Chen[2], D. C. Papa[1], and R. Blundell[1]

[1]Harvard-Smithsonian Center for Astrophysics,
60 Garden St., Cambridge, MA 02138

[2]Institute of Astronomy and Astrophysics
Academia Sinica, Taipei, Taiwan 115

ABSTRACT

We report on a novel radio-wave alignment technique for millimeter and sub-millimeter wavelength receiving systems of radio astronomy. The technique employs a near-field scanning system to map out the 2-D amplitude and phase beam profile of a receiving system under test. Next, small scatterers, such as a pair of cross-wires or small absorbers, are introduced at known locations between the transmitting scanner and the receiver. The resultant beam pattern is measured again. These small scatterers ideally do not introduce substantial perturbation in the measured amplitude pattern. A full-wave, numerical method is then applied to transform the measured field onto the plane of the scatterers. By comparing the transformed field distributions with and without the scatterers, we can determine whether the beam is physically displaced or tilted in some ways, thereby, providing diagnosis to the alignment of different optical components in a receiving system. We will describe the application of this technique to verify the alignment of the receiver optics of the 200 GHz receivers of the Sub-Millimeter Array. The limitations of the method will also be discussed.

Keywords: Radio-wave alignment, near-field measurement, near-field numerical simulation, the Sub-millimeter Array.

I. INTRODUCTION

Aligning receiver and optical components is one of the most basic tasks in telescope operation. A well-aligned receiving system will yield optimal coupling to the incoming signal beam while a poorly aligned system will cause degrade overall system efficiency and performance. Compared to optical telescopes, aligning components of a radio telescope is more difficult because non-optical devices are commonly used in radio systems. For example, wire grids can be used as polarizer or diplexer and they are not good reflectors for visible light. Teflon is used in vacuum windows or lenses for its transparency to mm and sub-mm wavelength signal, but it is opaque to visible light. The presence of such components in a receiving system makes it rather difficult to carry out a complete system alignment using standard optical alignment techniques with laser beams.

In this report, we demonstrate a radio-alignment technique useful for millimeter and sub-millimeter receiving system. This technique employs a near-field scanning system to map out the 2-D power and phase beam profiles. Unlike optical alignment with laser system, near-field scanning is slow. It is therefore not possible to perform real-time alignment using near-field scanning data. In order to make maximum use of the measured data, we have developed a novel diagnostic procedure. Scatterers, such as a pair of cross-wires or small absorbers, are introduced at known locations between the receiver and the near-field scanner. The measured vector field at the scanning plane is transformed onto the plane of scatterers using a full-wave, numerical Kirchhoff integral. By comparing the transformed field with and without the scatterers we can determine the degree of alignment of the receiving system-- beam tilt, lateral displacement of the beam from the optical axis, and longitudinal displacement due to change in focal length. Using different scatterers placed at different locations, it is possible to infer the source of misalignment and devise ways to correct it.

This paper reports on the application of such technique to verify the alignment of the receiver optics of the 200 GHz receivers of the Sub-Millimeter Array (SMA). It firstly describes the SMA receiver optics, along with the near-field measurement setup. The Kirchhoff integral is introduced next. Then the measured beam pattern and subsequent data analysis are presented. Finally, the accuracy and limitation of this method is discussed.

II. RECEIVER OPTICS & SCANNING SETUP

The Submillimeter Array (SMA), currently under construction by the Smithsonian Astrophysical Observatory (SAO) and the Institute of Astronomy and Astrophysics of Academia Sinica in Taiwan, will function as a fully automated radio interferometer of eight 6-m antennas. Fixed-tuned receivers incorporating superconductor-insulator-superconductor (SIS) mixers are being developed to cover the major submillimeter atmospheric windows from 176 GHz to 900 GHz.[1-6] Figure 1 shows the optics layout for the receiver system in lower frequency bands. The design of the lens and feed combination in different frequency bands creates an identical virtual feed at a distance 780mm behind the lens.[6] The lens is located at the 80K shield, and the mixer is at the 4K stage of the cryostat.

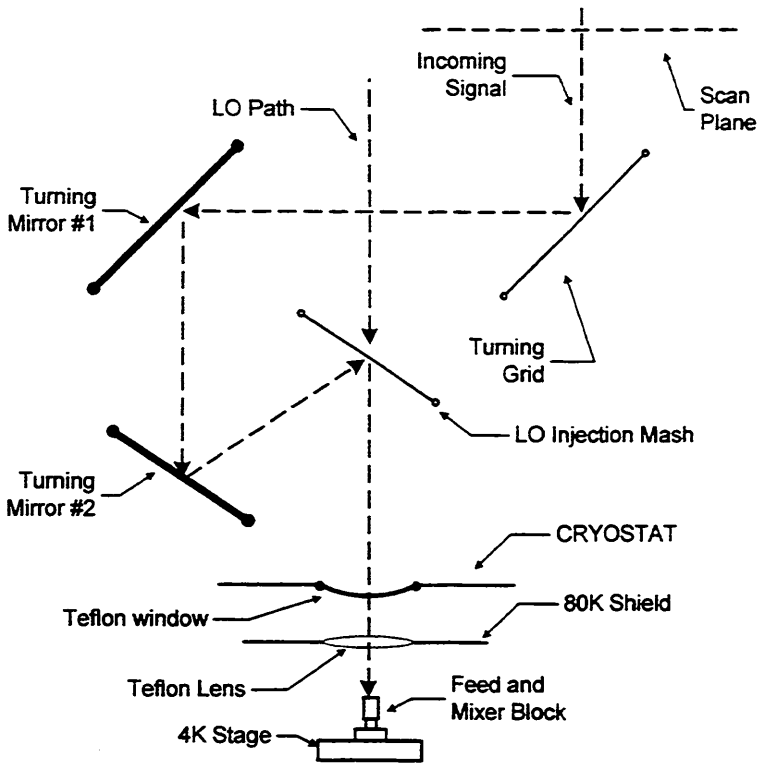

Figure 1: Schematic diagram of the SMA receiver optics.

Initial system alignment is performed optically with lasers by replacing the grid and the mesh with optical beam splitters. Once the optical alignment is done, we set up a near-field measurement system to map out the beam patterns of each receiver insert under test. The scanner consists of an XY translation stage mounted on top of the receiver system perpendicular to the signal path. A high-frequency transmitter set up on the translation stage is used as a signal source. Total radiated power coupled to the SIS junction is well below the saturation level of the mixer. The master reference signal for the entire system is the 10 MHz internal reference of a signal synthesizer.

The transmitter is tuned to operate at 242 GHz for the 200 GHz band receiver. A dynamic range of more than 50 dB, and short-term phase fluctuation of less than 5 degrees are achieved with the current setup. The scan area is typically 120 mm X 120 mm. The scanning time is mainly limited by the speed of the stepper motor. In a typical scan with sampling points 1.5 mm apart on an 81 X 81 mesh, total scan time is around 100 minutes. No probe correction has been applied to the measured data because the beams are essentially paraxial.

Special precautions have been taken to ensure that the scan plane is normal to the optical axis of the receiver assembly. We have measured that the scan plane is parallel to the top plate of the receiver assembly to within 50 μm over a distance of 150 mm. Long-term phase fluctuation has also been measured and it is typically less than 3

degrees RMS at 240 GHz over a measurement period. This is equivalent to about 10 μm, over a distance of 150 mm. This error is considered as an additional alignment error. Combined with the positioning error of the probe, we have a total misalignment budget of 60μm over the 150 mm scan plane, equivalent to a maximum pointing error of 1.4 arc minutes.

III. NUMERICAL METHOD

The numerical calculation is based on a Kirchhoff integral in the following form:[7]

$$\vec{E}(\vec{r}) = \frac{1}{2\pi}\int_S \frac{e^{ikR}}{R^2}\left[jk - \frac{1}{R}\right]\cdot \vec{R}\times\left[\hat{z}\times\vec{E}(\vec{r}_0)\right]\cdot dS \qquad (1)$$

where k is the propagation constant, $\hat{z}$ the unit normal vector of the plane defined by $\vec{r}_0$, and $\vec{R} = \vec{r} - \vec{r}_0$. Using the above formalism, we have developed a computer code to calculate the electric field, $\vec{E}(\vec{r})$, on a target plane of interest (scatter plane) from an initial plane with known field distribution, $\vec{E}(\vec{r}_0)$.

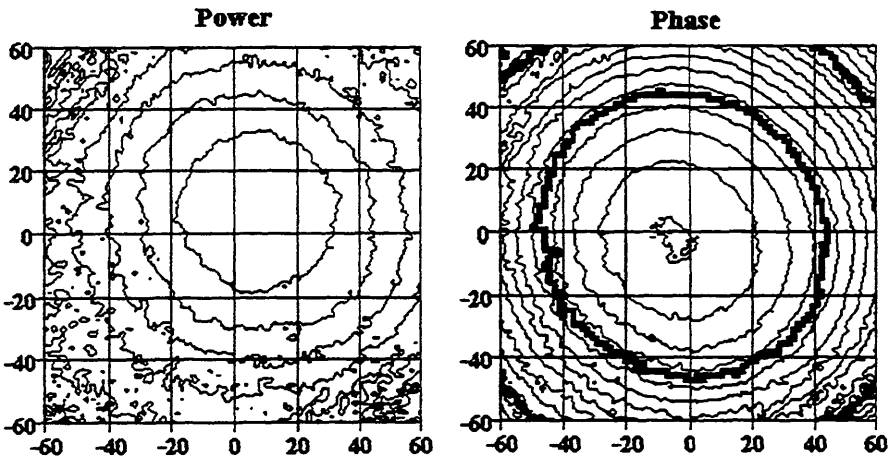

Figure 2: Beam pattern of the 200 GHz receiver measured at 242 GHz. The power contours are every 5 dB descending from the origin, while the phases are every 50 degrees. The dimensions are in millimeters.

IV. BEAM PATTERNS AND ALIGNMENT

In Fig. 2 we show the beam patterns of the 200 GHz receiver measured at 242 GHz. Obviously, the beam is misaligned with the beam center being displaced by about 10mm from the optical axis. The fact that the power and the phase maxima locate at different positions implies that the beam is actually tilted. It is not clear from this data set where the misalignment is introduced. To solve this problem, we have

performed a second scan with a cross-wire introduced at a location between the turning grid and the turning mirror #1, at a distance of 370mm from the scan plane. The diameter of the wire is 1.2 mm. The measured fields, with and without the cross-wire, are then transformed back to the scatterer plane. The difference of the 2 amplitude patterns on the scatterer plane reveals the cross-wire (see Figure 3). From this 2-D differential amplitude map, we can clearly see the center of the cross, which is about 1 mm away from the optical axis. This slight deviation is due to the thickness of the cross-wire. Since this error is small compared to the 10mm offset of the beam center shown in Fig.2. We can therefore conclude that the rotating grid is not the cause of the displacement of the beam.

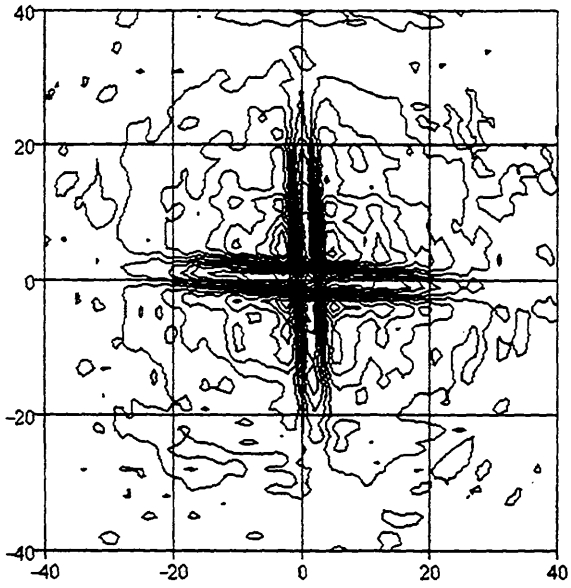

FIGURE 3. Differential amplitude contours showing a cross-wire in the signal path.

We have attempted to inspect the entire room temperature optics by placing the cross-wires right at the vacuum window, about 1400 mm away from the scan plane. However, in this case the cross-wire is not well resolved, and its center remains undetermined. The reason is that the scan area is not sufficiently large considering the long distance between the scan plane and the scatterer. A small measurement area means that part of the evanescent wave generated by the scatterer falls outside the scan area. In order to determine the relation between the scan area and the scan distance, we have simulated numerically a case in which an absorber strip 4 mm wide is introduced at the vacuum window of the cryostat. The blocked field is transformed to several planes at different distances from the window. These data sets are calculated over finite area, corresponding to a limited scan size in the near-field measurement data set. The size of the scan area is initially chosen to cover the first side lobe of the beam. The simulated measurements are then transformed back to the absorber strip plane again to reconstruct the image of the absorber strip. The results of

these simulations are shown in Fig. 4 as a cross-sectional view through the center of the window. Figure 4A shows that when the scan plane is more than 500 mm from the scatterer plane, we would not be able to resolve the absorber strip. We further explore the size effect of the scan area. In a second simulation, the scan distance is fixed at 500mm, while the scan area is increased from 100 mm square to 200 mm and 300 mm square. The result shows that a larger scan area indeed improve the image resolution. The cross-sectional view of the simulated images are shown in Fig. 4b.

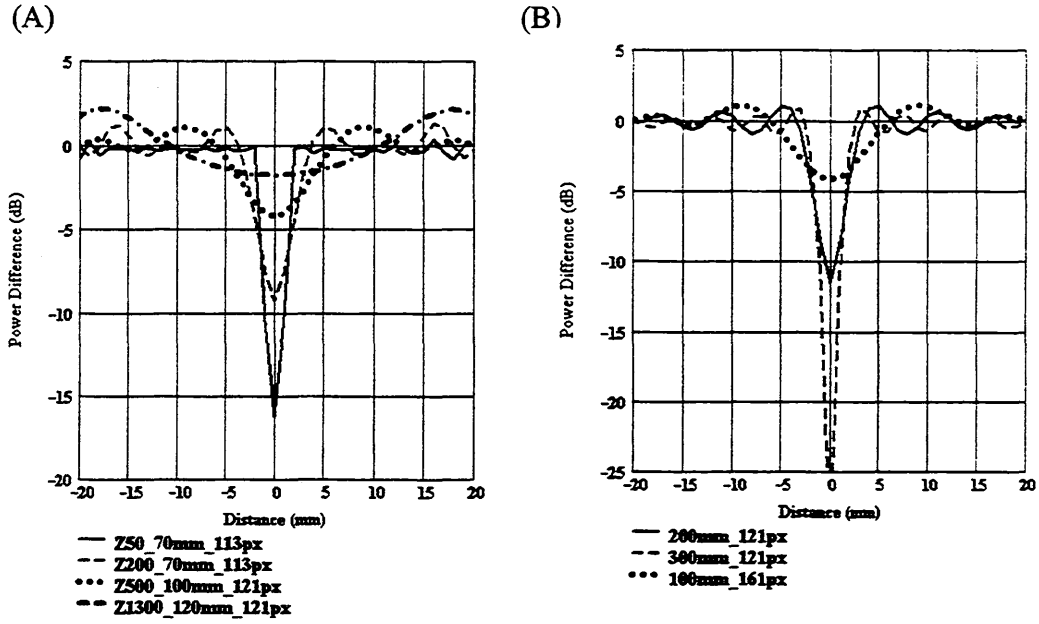

Figure 4: Cross-sectional view of the reconstructed absorber strip at the vacuum window. The traces are labeled according to the distance and size of the "scan" planes: "Z" indicates distance from the window to the scan plane, "mm" the width of the scan area, and "px" the number of sample points along one side. Figure (B) is generated from a plane located 500 mm from the window in the optical path.

Owing to the limitation of our measurement equipment and the physical system layout, a larger scan area is not achievable. Thus we have tried a different scheme of scatterer arrangement. A pair of small absorbers are introduced at diametrically positions about the center of the vacuum window which is also the optical axis. They are placed in a region of moderate beam power, about -10 to -15 dBc. Once again we measure the beam profile with and without the absorbers, and compute a differential amplitude map at the plane of the absorbers. Two such maps are shown in Fig. 5. The centers of the scatters are determined by fitting the image contours to a bi-quadratic function. The intersection of the lines connecting each pair of absorbers gives the mechanical center of the vacuum window in the image. From these images, the mechanical center

is found to be 2mm (∀0.5mm) from the beam center at the dewar window. This result verifies the alignment of the receiver optics between the vacuum window and the turning wire-grid to be within 5 arc-minutes. This small error may be due to uncertainties introduced in the fitting process. From this result, we conclude that the cause of the beam misalignment is inside the cryostat.

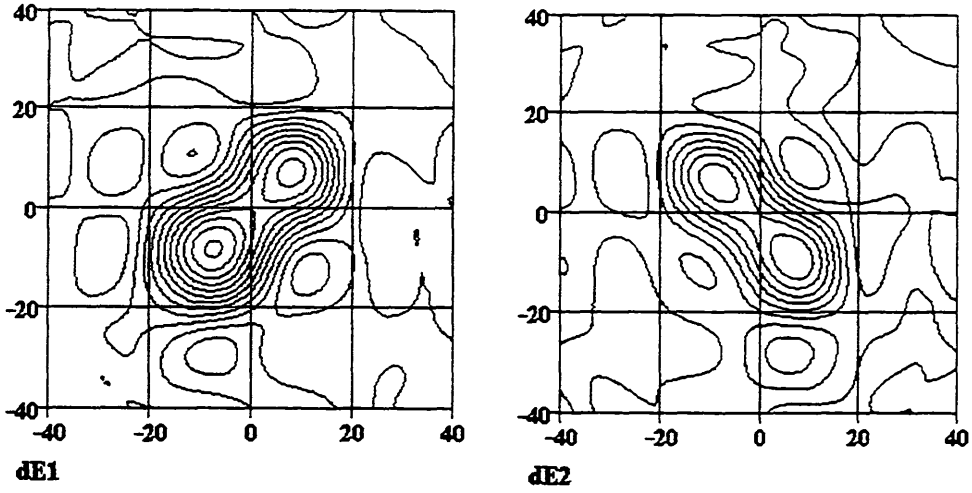

Figure 5: Differential amplitude maps showing a pair of absorbers placed at the vacuum window. The two most prominent peaks in each image correspond to the pair of small, circular absorbers. The amplitude contours are in 0.01 steps. The dimensions are in millimeters.

V. SUMMARY

We have demonstrates a radio-wave alignment technique for mm and sub-mm wavelength receiver system. This method is very useful in the alignment of mm and sub-mm telescope and receiver system with complicated optics design. We have applied the technique to verify the alignment of the SMA receiver optics. This technique has the advantage of providing an *in situ* access to individual component in a complex, radio-wavelength receiving system. With careful design, we believe that we can perform a precise radio alignment diagnosis.

VI. ACKNOWLEDGMENT

The authors would like to thank Dr. Scott Paine for valuable discussion and Mr. Michael Smith for his superior technical assistance in aligning the receiver optics. Funding for MTC is supported in part by the National Science Council of Taiwan under a grant NSC-87-2213-E-001-028.

VII. REFERENCES

1. R. Blundell, C.-Y. E. Tong, D. C. Papa, R. L. Leombruno, X. Zhang, S. Paine, J. A. Stern, H. G. LeDuc, and B. Bumble, "A Wideband Fixed-Tuned SIS Receiver for 200-GHz Operation," IEEE Trans. Microwave Theory Tech., **MTT-43**, pp.933-937, 1995.

2. R. Blundell, C.-Y. E. Tong, J. W. Barrett, J. Kawamura, R. L. Loembruno, S. Paine, D. C. Papa, X. Zhang, J. A. Stern, H. G. LeDuc, and B. Bumble, "A Fixed Tuned Low Noise SIS Receiver for the 450 GHz Frequency Band," Proc.6th Int. Symp. Space Terahertz Tech. 1995.

3. C.-Y. E. Tong, R. Blundell, S. Paine, D. C. Papa, J. Kawamura, X. Zhang, J. A. Stern, and H.G. LeDuc, "Design and Characterization of a 250-350 GHz Fixed-Tuned Superconductor-Insulator-Superconductor Receiver," IEEE Trans. Microwave Theory Tech. **MTT-44**, pp. 1548-1556, 1996.

4. C.-Y. E. Tong, R. Blundell, D. C. Papa, J. W. Barrett, S. Paine, X. Zhang, J. A.Stern, and H. G. LeDuc, "A Fixed Tuned Low Noise SIS Receiver for the 600 GHz Frequency Band," Proc. 6th Int. Symp. Space Terahertz Tech. 1995.

5. M. T. Chen, C. E. Tong, S. Paine, and R. Blundell, "Characterization of Corrugated Feed Horns at 216 and 300 GHz", International Journal of Infrared and Millimeter Waves, Vol. 18, No.9, pp. 1697-1710, 1997.

6. S. Paine, D. C. Papa, R. L. Leombruno, X. Zhang, and R. Blundell, "Beam Waveguide and Receiver Optics for the SMA," Proc. 5th Int. Symp. Space Terahertz Tech. 811-823, 1994.

7. Thorkild B. Hansen and Arthur D. Yaghjian, "Planar Near-Field Scanning in the Time Domain, Part 1: Formulation," IEEE Tans. Antennas Propagat., AP-42, No.9, pp. 1280-1291, 1994.